CHAPTER V

THE LORENZ MODEL FOR ATMOSPHERIC CIRCULATION

In this chapter we will study about some applications of the *Lorenz model* for the atmospheric circulation. In this study we will regard the flow of the atmosphere as a quasi-stationary circulation of large scale on which are superimposed transient wave and vortex disturbances of smaller scale originating as instabilities of the mean flow and interacting with it.

Model Equations

The actual atmosphere is of course baroclinic, but all of the phenomena to be considered have their counterparts in the simpler barotropic atmosphere. Thus questions involving topographic forcing, resonance and nonlinear interaction via the advective terms in the equations of motion may be studied barotropically. For example, the prototypical quasi-equilibrium phenomenon of blocking has been found by Egger [Egger 1978] in numerical simulations of the flow of barotropic atmosphere over topography. It is true that such phenomena as baroclinic instability and vertical propagation of energy are not present in a barotropic model, but the former occurs on scales that are smaller than those we wish to study, and the latter does not occur when the waves are trapped vertically as by easterlies or strong westerlies [Charney and Drazin 1961, Charney 1969]. Baroclinic instability may be important in the present context only as additional forcing of the planetary-scale motions.

We will therefore take our model as a homogeneous β-plane atmosphere with a free surface of height $H + \eta$ and the mean height H confined between zonal walls of a distance πL. The lower boundary elevation will be denoted by h (x, y), where x is the eastward directed coordinate and y is the northward directed coordinate.

Since the motions will be on large scale, they will be quasi-geostrophic and therefore governed by the conservation of potential vorticity [Charney and Devore 1979]

$$\frac{\partial}{\partial t}\left(\nabla^2\psi - \frac{\psi}{\lambda^2}\right) + J\left(\psi, \nabla^2\psi - \frac{\psi}{\lambda^2} + f_0\frac{h}{H} + \beta y\right) = -f_0\frac{D_E}{2H}\nabla^2(\psi - \psi^*), \tag{5.1}$$

with the boundary condition;

$$v(x, 0) = v(x, \pi L) = 0, \tag{5.2}$$

where u is the eastward component of $\vec{U}$,

v is the northward component of $\vec{U}$,

$\vec{\nabla}$ is the horizontal gradient operator,

J is the Jacobian operator;

$$J(F, G) \equiv \frac{\partial(F, G)}{\partial(x, y)} = \frac{\partial F}{\partial x}\frac{\partial G}{\partial y} - \frac{\partial G}{\partial x}\frac{\partial F}{\partial y},$$

f_0 is the Coriolis parameter ($f_0 = 2\Omega \sin \phi_0$),

$\beta = \frac{2\Omega \cos \phi_0}{a}$, $\lambda^2 = \frac{gH}{f_0^2}$; where

Ω is the angular speed of the Earths rotation,

a is the radius of the Earth,

ϕ_0 is a central latitude,

D_E is the Ekman depth ($D_E = \sqrt{2\nu_E/f_0}$; where

ν_E is the bulk eddy viscosity in the frictional boundary layer),

ψ is a stream function which satisfies

$$u = -\frac{\partial \psi}{\partial y} \quad \text{and} \quad v = \frac{\partial \psi}{\partial x}, \tag{5.3}$$

$$\zeta = \frac{\partial v}{\partial x} - \frac{\partial u}{\partial y} = \nabla^2 \psi , \tag{5.4}$$

In deriving Eq.(5.1), we assumed that $|h| << H$ and that $\pi L << 2a$. The motion is retarded by a frictionally induced vorticity sink given by $-f_0 w_E/H$, where w_E is the Ekman pumping, $\frac{D_E}{2} \nabla^2 \psi$. It is accelerated by the momentum source *(U, V)* giving rise to the vorticity source

$$\frac{\partial V}{\partial x} - \frac{\partial U}{\partial y} = \left(f_0 \frac{D_E}{2H}\right) \nabla^2 \psi^* , \tag{5.5}$$

In a baroclinic atmospheric *(U, V)* would be the thermal wind driven by the radiation field.

We now rewrite the variables of the problem in terms of non-dimensional variables as follows :

$t' = f_0 t$, $x' = x/L$, $y' = y/L$, $h' = h/H$, $\psi' = \psi/L^2 f_0$, and $\psi^{*'} = \psi^*/L^2 f_0$.

By the introduction of these transformations into Eq.(5.1) we obtain the non-dimensional equation

$$\frac{\partial}{\partial t'}\left(\nabla'^2 \psi' - \frac{\psi'}{\lambda'^2}\right) + J\left(\psi', \nabla'^2 \psi' - \frac{\psi'}{\lambda'^2} + f_0 \frac{h'}{H}\right) + \bar{\beta} \frac{\partial \psi'}{\partial x'} + k \nabla'^2 \left(\psi' - \psi^{*'}\right) = 0, \tag{5.6}$$

where $\bar{\beta} = (L/a) \cot \phi_0$, $\lambda'^2 = \dfrac{gH}{(f_0 L)^2}$,

$k = \dfrac{D_E}{2H} = \sqrt{E/2}$; where E is the Ekman number.

By omitting the notation $'$ in Eq.(5.6), it becomes

$$\frac{\partial}{\partial t}\left(\nabla^2 \psi - \frac{\psi}{\lambda^2}\right) + J\left(\psi, \nabla^2 \psi - \frac{\psi}{\lambda^2} + h\right) + \bar{\beta} \frac{\partial \psi}{\partial x} + k \nabla^2 \left(\psi - \psi^*\right) = 0, \tag{5.7}$$

To simplify the Eq.(5.7) further, we expand ψ, ψ^* and h in orthogonal trigonometric functions. This procedure closely parallels that of Lorenz [Lorenz 1963] who derived similar spectral equations for a two-layer channel flow model. Our equations differ from his only in applying to a single layer and in including the effects of topography, driven force and variations of the Coriolis parameter. Like Lorenz, the expansion of ψ had been truncated to include a total of three terms only. Accordingly, in this study we let

$$\psi = \psi_1 F_1 + \psi_2 F_2 + \psi_3 F_3 , \tag{5.8}$$

where ψ_1, ψ_2 and ψ_3 are functions of time alone,

$F_1 = \sqrt{2} \cos y$, $F_2 = 2 \cos (nx) \sin y$, $F_3 = 2 \sin (nx) \sin y$;

n is a positive integer.

Likewise, we can obtain that

$$\psi^* = \psi_1^* F_1 + \psi_2^* F_2 + \psi_3^* F_3 , \tag{5.9}$$

and

$$h = h_1 F_1 + h_2 F_2 + h_3 F_3 . \tag{5.10}$$

When expressions (5.8), (5.9) and (5.10) are substituted into Eq.(5.7), we obtain the equations

$$\begin{aligned} \frac{dX}{dt} &= -k_{n0}\left(X - \psi_1^*\right) + h_{n0}^*(h_2 Z - h_3 Y) , \\ \frac{dY}{dt} &= -k_{n1}\left(Y - \psi_2^*\right) - \left(\alpha_{n1} X - \beta_{n1}\right) Z - h_{n1}^*(h_3 X - h_1 Z) , \\ \frac{dZ}{dt} &= -k_{n1}\left(Z - \psi_3^*\right) + \left(\alpha_{n1} X - \beta_{n1}\right) Y + h_{n1}^*(h_1 Y - h_2 X) , \end{aligned} \tag{5.11}$$

where $X \equiv \psi_1$, $Y \equiv \psi_2$, $Z \equiv \psi_3$,

$$h_{n0}^* = \frac{2n\sqrt{2}}{1 + \lambda^{-2}} , \qquad h_{n1}^* = \frac{n\sqrt{2}}{n^2 + 1 + \lambda^{-2}} ,$$

$$\alpha_{n1} = \frac{n^3\sqrt{2}}{n^2 + 1 + \lambda^{-2}} , \qquad \beta_{n1} = \left(\frac{n}{n^2 + 1 + \lambda^{-2}}\right)(L/a) \cot \phi_0 ,$$

$$k_{nm} = \left(\frac{n^2 + m^2}{n^2 + m^2 + \lambda^{-2}}\right) k ; \qquad m = 0 \text{ and } 1.$$

Eq.(5.11) is so-called the *"Lorenz Model for Atmospheric Circulation"*. What can such a simple model possibly tell us about the real atmosphere? Certainly it cannot yield much quantitative information. It may serve principally in examining existing hypotheses and formulating new ones. Often we draw conclusions about the general circulation on the basis of qualitative reasoning. Sometimes we can apply similar reasoning to the model, and, in addition, we can solve the equations of the model. If the solution fits the reasoning, it will give us added confidence in our reason-ing regarding the real atmosphere. If it reveals a flaw in the reasoning, it will indicate where our reasoning in the atmospheric case needs reexamination.

Analysis of the Model

Assuming the topographical effect of the stretching and compression of the vortex tubes of the Earth's rotation to be confined to the toposphere, we set $H = 10^4$ m as an approximation to the height of the topopause. If it were desired to simulate accurately as possible the phase velocity of the dominant free or forced Rossby wave modes in a baroclinic atmosphere with the observed vertical density structure, the acceleration of gravity g should be chosen so as to give the correct *equivalent height* for the actual atmosphere. In the case of traveling free Rossby waves the results of Diky and Golitsyn [Diky and Golitsyn 1968] suggest $4\,\Omega^2 a^2/gH = 8.8$, or $g = 3.6$ m sec^{-2} for $H = 10^4$ m. It will be more convenient to set $g \to \infty$ and $\lambda^{-2} = 0$, i.e., to replace the upper free surface by a rigid horizontal boundary.

For simplicity and to ensure that we are dealing with large topographic scales, we consider only wavelike topography mode 2. Thus

$$h \;=\; h_2 F_2 \;=\; \left(\frac{h_0}{H}\right) \cos(nx) \sin y\,, \tag{5.12}$$

where h_0 is arbitrary.

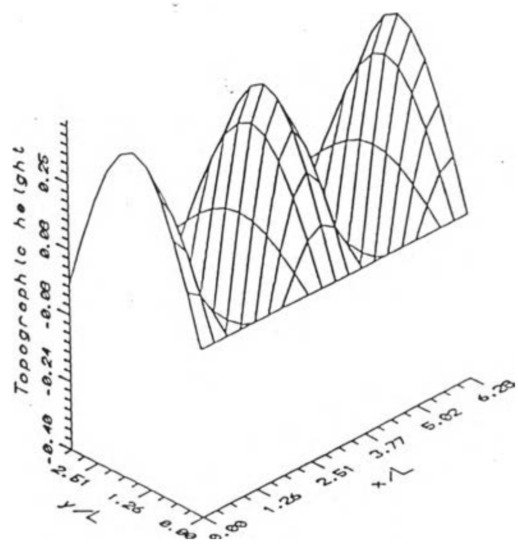

Figure 5.1 Wavelike topography for n = 2 and $h_0/H = 0.20$; h = 0.40 cos 2x sin y.

Substituting this expression into Eq.(5.11), we obtain the equations

$$\frac{dX}{dt} = -k_{n0}\left(X - \psi_1^*\right) + h_{n0} Z ,$$

$$\frac{dY}{dt} = -k_{n1}\left(Y - \psi_2^*\right) - \left(\alpha_{n1}X - \beta_{n1}\right)Z , \qquad (5.13)$$

$$\frac{dZ}{dt} = -k_{n1}\left(Z - \psi_3^*\right) + \left(\alpha_{n1}X - \beta_{n1}\right)Y - h_{n1}X ,$$

Here $h_{n0} = h_{n0}^* h_2 = h_{n0}^*\left(\frac{h_0}{2H}\right)$ and $h_{n1} = h_{n1}^* h_2 = h_{n1}^*\left(\frac{h_0}{2H}\right)$.

We now examine some properties of the Eqs.(5.13) by splitting them into some special cases as follows :

A. Conservative Flow

We first consider the conservative case by setting ψ^* and k equal to zero. Then the system will be governed by

$$\frac{dX}{dt} = h_{no} Z ,$$

$$\frac{dY}{dt} = -\left(\alpha_{n1}X - \beta_{n1}\right)Z , \qquad (5.14)$$

$$\frac{dZ}{dt} = \left(\alpha_{n1}X - \beta_{n1}\right)Y - h_{n1}X ,$$

Some properties of Eqs.(5.14) are examined as follows:

1. Divergence of the Flow; D

By introduction of the divergence; D, into Eqs.(5.14) we find that D = 0. Thus

$$\Gamma(t) = \Gamma(0), \tag{5.15}$$

where $\Gamma(0)$ is an element of phase-space volume at the time t = 0,

$\Gamma(t)$ is an element of phase-space volume at the time t.

Hence the expansion rate change of phase-space volume equal to zero.

2. Steady-state Solutions or Equilibrium States

We now consider steady-state solutions of Eqs.(5.14). Equating the time derivatives to zero. We find that

$$Y_0 = h_{n1}X_0/(\alpha_{n1}X_0 - \beta_{n1}) \qquad \text{and} \qquad Z_0 = 0,$$

where X_0 is arbitrary, and

(X_0, Y_0, Z_0) is a steady-state solution or an equilibrium state of the system.

Table 5.1 Equilibrium states of a conservative flow for L/a = 1/4, and n = 2.

ϕ_0	h_0/H	X_0	Y_0	Z_0
45°	0.00	0.100000	0.000000	0.000000
	0.05	0.100000	0.055989	0.000000
	0.20	0.100000	0.223957	0.000000
	0.25	0.100000	0.280026	0.000000
	0.30	0.100000	0.336015	0.000000
	0.35	0.100000	0.392004	0.000000
	0.40	0.100000	0.447993	0.000000

Streamfunction fields satisfying the spectral model in Eq.(5.8) for some examples of equilibrium states of a conservative flow will be shown in Fig.(5.2).

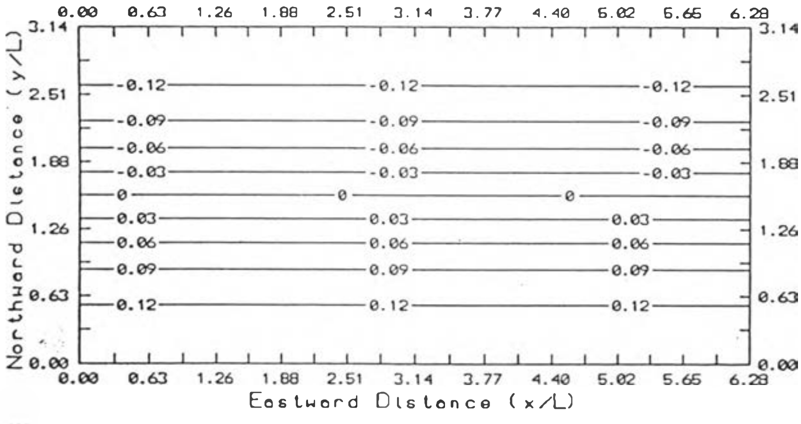

(a)

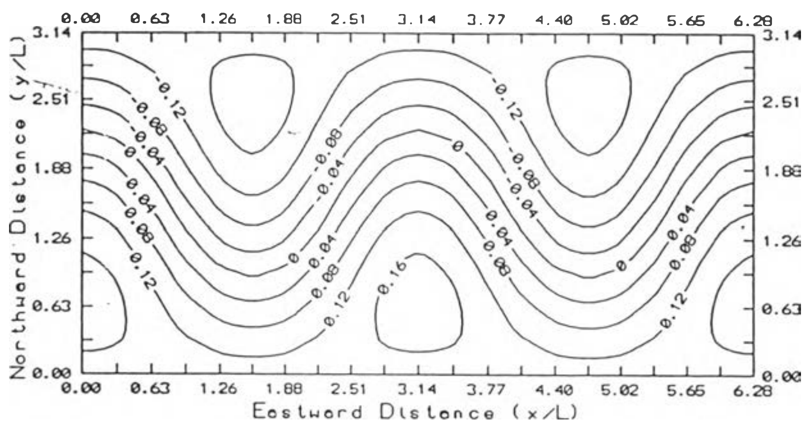

(b)

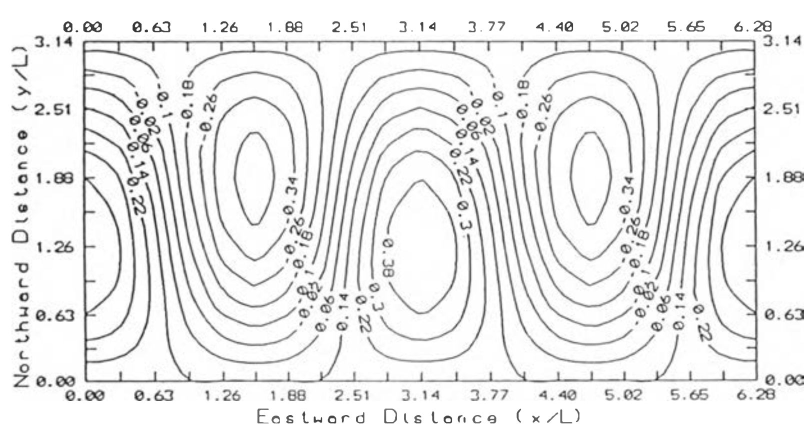

(c)

Figure 5.2 Streamfunction fields of the equilibrium states of a conservative flow for $\phi_0 = 45^{\circ}$, L/a = 1/4, n = 2, and

(a) $h_0/H = 0$ (b) $h_0/H = 0.05$ (c) $h_0/H = 0.20$.

3. Stability of the Equilibrium States

From the linearized transformation (See Appendix C), the stability matrix of an equili-brium state (X_0, Y_0, Z_0); M_0, will be obtained

$$M_0 = \begin{pmatrix} 0 & 0 & h_{n0} \\ 0 & 0 & -b_{n1} \\ B_{n1} & b_{n1} & 0 \end{pmatrix}, \qquad (5.17)$$

where $b_{n1} = \alpha_{n1}X_0 - \beta_{n1}$, and $B_{n1} = \alpha_{n1}Y_0 - h_{n1}$,

and thus, in greater detail;

$$\lambda_1 = 0, \quad \text{and} \quad \lambda_{2,3} = \sqrt{\frac{\beta_{n1}h_{n0}h_{n1} - b_{n1}^3}{b_{n1}}}.$$

Here λ_i are eigenvalues of the matrix M_0 ($i = 1, 2$ and 3).

To examine the stability property of the equilibrium states, we need to know the values of λ_i. We then can examine the stability of the equilibrium state as follows:

Case i: If $b_{n1} > 0$ and $\beta_{n1}h_{n0}h_{n1} > b_{n1}^3$, we find that $\lambda_{2,3} = \pm\mu$. Here μ is a positive value and

$$\mu = \sqrt{\frac{\beta_{n1}h_{n0}h_{n1} - b_{n1}^3}{b_{n1}}}.$$

Hence that the equilibrium state (X_0, Y_0, Z_0) is a *hyperbolic* one.

Case ii: If $b_{n1} > 0$ and $\beta_{n1}h_{n0}h_{n1} < b_{n1}^3$, we find that $\lambda_{2,3} = \pm i\omega$. Here ω is a positive value and

$$\omega = \sqrt{\frac{b_{n1}^3 - \beta_{n1}h_{n0}h_{n1}}{b_{n1}}}.$$

Hence that the equilibrium state (X_0, Y_0, Z_0) is an *elliptic* one.

Case iii: If $b_{n1} < 0$, we find that $\lambda_{2,3} = \pm i\omega^*$. Here ω^* is a positive value and

$$\omega^* = \sqrt{\frac{|b_{n1}^3| + \beta_{n1}h_{n0}h_{n1}}{|b_{n1}|}}.$$

Hence that the equilibrium state (X_0, Y_0, Z_0) is also an *elliptic* one.

B. Topographically and Thermally Driven Flow

Introduce zonal driving and dissipation in the first y-mode by setting $\psi^* = \psi_1^* F_1$. Here ψ_1^* is the driving Rossby number $U_0/(\sqrt{2}\, Lf_0)$, where U_0 is the dimensional amplitude of the forcing zonal wind profile. Substituting ψ^* into Eqs.(5.13), the system will be then governed by

$$\begin{aligned} \frac{dX}{dt} &= -k_{n0}\left(X - \psi_1^*\right) + h_{n0} Z, \\ \frac{dY}{dt} &= -k_{n1} Y - \left(\alpha_{n1} X - \beta_{n1}\right) Z, \\ \frac{dZ}{dt} &= -k_{n1} Z + \left(\alpha_{n1} X - \beta_{n1}\right) Y - h_{n1} X, \end{aligned} \tag{5.18}$$

Some properties of Eqs.(5.18) are examined as follows:

1. Divergence of the Flow; D

By introduction of the divergence; D, into Eqs.(5.18) we find that $D = -(k_{n0} + 2k_{n1})$. D is negative since k_{n0} and k_{n1} are positive. We thus have a contraction of the form

$$\Gamma(t) = \Gamma(0)\, exp\left[-(k_{n0} + 2k_{n1})\, t\right], \tag{5.19}$$

Hence all trajectories will ultimately become confined to some form of limiting manifold of volume zero.

2. Steady-state Solutions or Equilibrium States

We now consider steady-state solutions of Eqs.(5.18). Equating the time derivatives to zero. We find that

$$Y_0 = \left(\frac{h_{n1} b_{n1}}{b_{n1}^2 + k_{n1}^2}\right) X_0,$$

$$Z_0 = -\left(\frac{h_{n1} k_{n1}}{b_{n1}^2 + k_{n1}^2}\right) X_0,$$

while X_0 satisfies the cubic equation

$$\left(X_0 - \psi_1^*\right)\left(b_{n1}^2 + k_{n1}^2\right) + \left(\frac{h_{n0}h_{n1}k_{n1}}{k_{n0}}\right)X_0 = 0, \qquad (5.20)$$

Here $b_{n1} = \alpha_{n1}X_0 - \beta_{n1}$.

Table 5.2 Equilibria of a topographically and thermally driven flow for $\phi_0 = 45°$, $L/a = 1/4$, $n = 2$, $k = 10^{-2}$ and $h_0/H = 0.05$.

ψ_1^*	X_0	Y_0	Z_0
0.05	0.015253	- 0.016092	- 0.002457
0.10	0.021497	- 0.028513	- 0.005552
0.15	0.024955	- 0.038498	- 0.008843
0.20	0.027221	- 0.046929	- 0.012219
	0.080004	0.068762	- 0.008486
	0.181164	0.041285	- 0.001332
0.30	0.030112	- 0.060821	- 0.019087
	0.067618	0.087100	- 0.016434
	0.290660	0.036837	- 0.000661
0.40	0.031949	- 0.072124	- 0.026029
	0.062733	0.100050	- 0.023852
	0.393708	0.035191	- 0.000445
0.50	0.033259	- 0.081682	- 0.033009
	0.059884	0.110495	- 0.031126
	0.495247	0.034304	- 0.000336

Table 5.3 Equilibria of a topographically and thermally driven flow for $\phi_0 = 45°$, $L/a = 1/4$, $n = 2$, $k = 10^{-2}$ and $h_0/H = 0.20$.

ψ_1^*	X_0	Y_0	Z_0
0.05	0.002645	- 0.007868	- 0.000837
0.10	0.004790	- 0.015003	- 0.001683
0.15	0.006582	- 0.021572	- 0.002535
0.20	0.008113	- 0.027687	- 0.003391
0.30	0.010619	- 0.038854	- 0.005114
0.40	0.012608	- 0.048931	- 0.006846
0.50	0.014245	- 0.058177	- 0.008585
	0.172327	0.167893	- 0.005791
	0.401818	0.140407	- 0.001735
0.70	0.016814	- 0.074803	- 0.012074
	0.127515	0.190741	- 0.010117
	0.644061	0.134184	- 0.000989
0.90	0.018773	- 0.089585	- 0.015574
	0.110025	0.207954	- 0.013961
	0.859593	0.131754	- 0.000714

Streamfunction fields satisfying the spectral model in Eq.(5.8) for some examples of equilibrium states of a topographically and thermally driven flow for $\phi_0 = 45°$, $L/a = 1/4$, $n = 2$, $k = 10^{-2}$ and $h_0/H = 0.05, 0.20$ will be shown in Fig.(5.3) - (5.4).

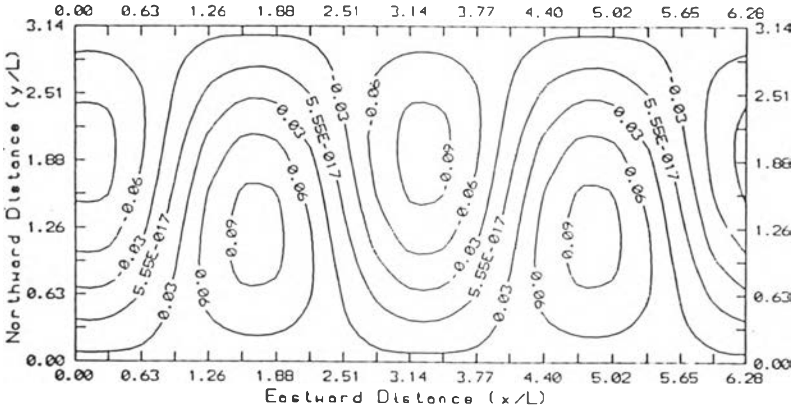

(a)

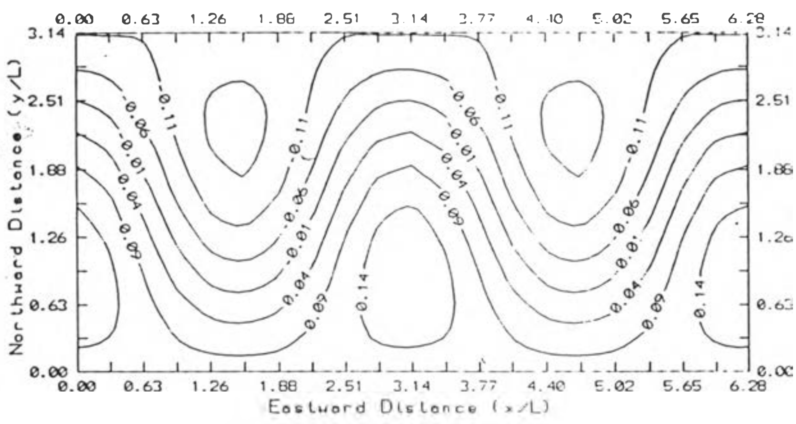

(b)

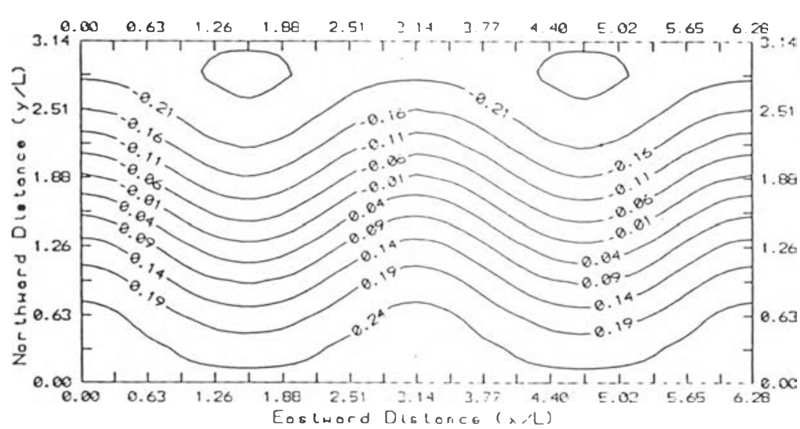

(c)

Figure 5.3 Streamfunction fields of the equilibria of a topographically driven flow for $\phi_0 = 45°$, $L/a = 1/4$, $n = 2$, $h_0/H = 0.05$, $k = 10^{-2}$, $\psi_1^* = 0.20$:
(a) $X_0 = 0.027221$ (b) $X_0 = 0.080004$ (c) $X_0 = 0.181164$

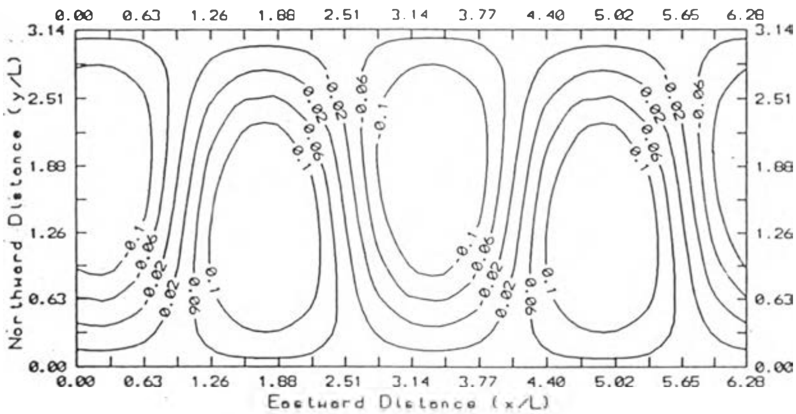

(a)

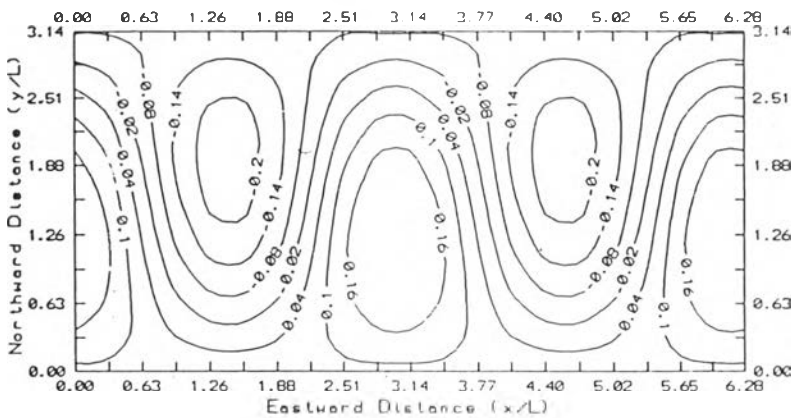

(b)

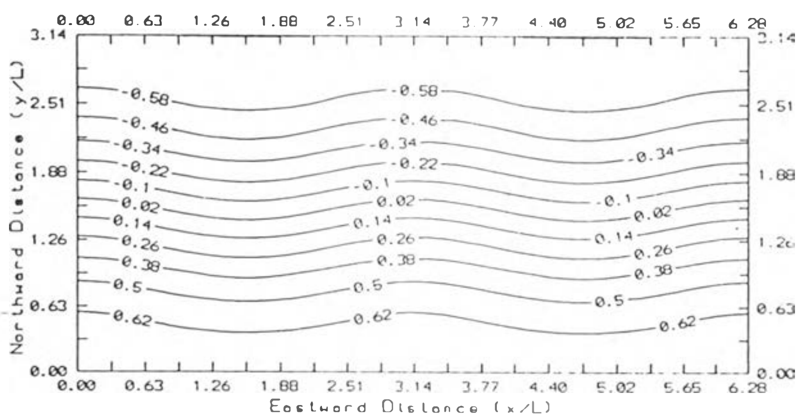

(c)

Figure 5.4 Streamfunction fields of the equilibria of a topographically driven flow for $\phi_0 = 45°$, $L/a = 1/4$, $n = 2$, $h_0/H = 0.05$, $k = 10^{-2}$, $\psi_1^* = 0.50$:
(a) $X_0 = 0.033259$ (b) $X_0 = 0.059884$ (c) $X_0 = 0.495247$

3. Stability of the Equilibrium States

From the linearized transformation (See Appendix C), the stability matrix of an equilibrium state (X_0, Y_0, Z_0); M_0, will be obtained

$$M_0 = \begin{pmatrix} -k_{n0} & 0 & h_{n0} \\ -\alpha Z_0 & -k_{n1} & -b_{n1} \\ B_{n1} & b_{n1} & -k_{n1} \end{pmatrix}, \tag{5.21}$$

and the eigenvalues of the stability matrix satisfy the cubic equation

$$\left(k_{n0} + \lambda_i\right)\left(k_{n1} + \lambda_i\right)^2 + \left(b_{n1}^2 - h_{n0}B_{n1}\right)\left(k_{n1} + \lambda_i\right) + h_{n0}b_{n1}\alpha_{n1} Z_0 = 0, \tag{5.22}$$

where λ_i are eigenvalues of the matrix M_0 (i = 1, 2 and 3),

$b_{n1} = \alpha_{n1}X_0 - \beta_{n1}$, and $B_{n1} = \alpha_{n1}Y_0 - h_{n1}$.

Rewrite Eq.(5.23) into the form

$$\lambda_i^3 + a_2\lambda_i^2 + a_1\lambda_i + a_0 = 0, \tag{5.23}$$

Here $a_0 = k_{n0}k_{n1}^2 + k_{n1}\left(b_{n1}^2 - h_{n0}B_{n1}\right) + h_{n0}b_{n1}\alpha_{n1}Z_0$,

$a_1 = k_{n1}^2 + 2k_{n0}k_{n1} + b_{n1}^2 - h_{n0}B_{n1}$,

and

$a_2 = k_{n0} + 2k_{n1}$.

To examine the stability property of the equilibrium states, we need to know the values of λ_i. If we let

$$q = \frac{1}{3}a_1 - \frac{1}{9}a_2^2 \quad \text{and} \quad r = \frac{1}{6}(a_1a_2 - 3a_0) - \frac{1}{9}a_2^3;$$

the solutions of Eq.(5.23) can be examined as follows:

Case i: If $q^3 + r^2 < 0$, we find that $\lambda_{1,2,3}$ are all real. Hence that the equilibrium state (X_0, Y_0, Z_0) may be a *stable*, *unstable* or *hyperbolic* one.

Case ii: If $q^3 + r^2 = 0$, we find that $\lambda_{1,2,3}$ are all real and at least two are equal - the case of degenerate roots. Hence that the equilibrium state (X_0, Y_0, Z_0) may be a *stable,* or *unstable improper* one.

Case iii: If $q^3 + r^2 > 0$, we find that λ_1 is real and $\lambda_{2,3}$ are a pair of complex conjugate roots. Hence that the equilibrium state (X_0, Y_0, Z_0) may be a *stable,* or *unstable spiral* one.

Numerical Experiments

To obtain numerically approximate solutions of Eqs.(5.13), we must choose numerical values of the parameters for our considerate systems. In this study, we will consider only the topographically and thermally driven flow for $\phi_0 = 45°$, $n = 2$, $k = 10^{-2}$, $L/a = 1/4$, $h_0/H = 0.05$ and $\psi_1^* = 0.20$. By substituting these parameters into Eqs.(5.13) we then obtain

$$\begin{aligned}\frac{dX}{dt} &= -0.01(X - 0.20) + 0.1414Z,\\ \frac{dY}{dt} &= -0.01Y - (2.262742X - 0.10)Z,\\ \frac{dZ}{dt} &= -0.01Z + (2.262742X - 0.10)Y - 0.0707X,\end{aligned} \tag{5.24}$$

We have used the *Euler-backward difference procedure* (See Appendix D) for ob-taining approximate solutions of Eq.(5.24). The value $\Delta t = 0.1$ has been chosen for the dimensionaless time increment. The computations have been performed on a IBM (PC/AT) 80386-25 compatible computer. For initial conditions we have been chosen a slight departure from the steady state of the flow. The results which have been prepared by the computor have been shown in the following tables. It gives the values of N (the number of iterations), X, Y and Z at every 500th for the first 5000 iterations.

Table 5.4 Numerical solutions of a topographically and thermally driven flow for $\phi_0 = 45°$, $n = 2$, $k = 10^{-2}$, $L/a = 1/4$, $h_0/H = 0.05$ and $\psi_1^* = 0.20$ with the initial condition (0.020000, -0.046000, -0.012000).

N	X	Y	Z
0000	0.020000	- 0.046000	- 0.012000
0500	0.027995	- 0.045885	- 0.007390
1000	0.029598	- 0.045382	- 0.013664
1500	0.025904	- 0.046741	- 0.013815
2000	0.026558	- 0.047138	- 0.011038
2500	0.027972	- 0.046693	- 0.011958
3000	0.027211	- 0.046811	- 0.012816
3500	0.026893	- 0.047021	- 0.012114
4000	0.027340	- 0.046921	- 0.012002
4500	0.027316	- 0.046881	- 0.012343
5000	0.027135	- 0.046944	- 0.012267

Table 5.5 Numerical solutions of a topographically and thermally driven flow for $\phi_0 = 45°$, $n = 2$, $k = 10^{-2}$, $L/a = 1/4$, $h_0/H = 0.05$ and $\psi_1^* = 0.20$ with the initial condition (0.020001, -0.046001, -0.012001).

N	X	Y	Z
0000	0.020001	- 0.046001	- 0.012001
0500	0.027995	- 0.045886	- 0.007390
1000	0.029598	- 0.045382	- 0.013664
1500	0.025905	- 0.046741	- 0.013815
2000	0.026558	- 0.047138	- 0.011038
2500	0.027972	- 0.046693	- 0.011958
3000	0.027211	- 0.046811	- 0.012816
3500	0.026893	- 0.047021	- 0.012114
4000	0.027340	- 0.046921	- 0.012002
4500	0.027316	- 0.046881	- 0.012343
5000	0.027135	- 0.046944	- 0.012267

Table 5.6 Numerical solutions of a topographically and thermally driven flow for $\phi_0 = 45°$, n = 2, k = 10^{-2}, L/a = 1/4, h_0/H = 0.05 and $\psi_1^* = 0.20$ with the initial condition (0.080000, 0.068762, -0.008486).

N	X	Y	Z
0000	0.080000	0.068762	- 0.008486
0500	0.079968	0.068773	- 0.008508
1000	0.078163	0.069392	- 0.009662
1500	- 0.053494	- 0.035493	- 0.049596
2000	- 0.032062	- 0.049911	- 0.015078
2500	0.009611	- 0.039906	0.025736
3000	0.046977	- 0.036999	0.002799
3500	0.035200	- 0.038013	- 0.027406
4000	0.016906	- 0.047641	- 0.016887
4500	0.026309	- 0.047277	- 0.004164
5000	0.031712	- 0.045225	- 0.012859

Table 5.7 Numerical solutions of a topographically and thermally driven flow for $\phi_0 = 45°$, n = 2, k = 10^{-2}, L/a = 1/4, h_0/H = 0.05 and $\psi_1^* = 0.20$ with the initial condition (0.080001, 0.068763, -0.008485).

N	X	Y	Z
0000	0.080001	0.068763	- 0.008485
0500	0.080080	0.068733	- 0.008437
1000	0.083966	0.067228	- 0.006084
1500	0.121695	0.047825	- 0.005713
2000	0.139595	0.046824	- 0.000391
2500	0.153683	0.044653	- 0.002060
3000	0.163169	0.043232	- 0.001708
3500	0.169418	0.042413	- 0.001334
4000	0.173572	0.041816	- 0.001319
4500	0.176202	0.041630	- 0.001425
5000	0.177905	0.041552	- 0.001366

Table 5.8 Numerical solutions of a topographically and thermally driven flow for ϕ_0 = 45°, n = 2, k = 10^{-2}, L/a = 1/4, h_0/H = 0.05 and ψ_1^* = 0.20 with the initial condition (0.181000, 0.041000, -0.001000).

N	X	Y	Z
0000	0.181000	0.041000	- 0.001000
0500	0.180946	0.041346	- 0.001538
1000	0.181024	0.041320	- 0.001240
1500	0.181096	0.041258	- 0.001365
2000	0.181101	0.041308	- 0.001326
2500	0.181134	0.041277	- 0.001331
3000	0.181140	0.041289	- 0.001335
3500	0.181151	0.041284	- 0.001330
4000	0.181156	0.041284	- 0.001333
4500	0.181159	0.041284	- 0.001332
5000	0.181160	0.041284	- 0.001332

Table 5.9 Numerical solutions of a topographically and thermally driven flow for ϕ_0 = 45°, n = 2, k = 10^{-2}, L/a = 1/4, h_0/H = 0.05 and ψ_1^* = 0.20 with the initial condition (0.181001, 0.041001, -0.001001)).

N	X	Y	Z
0000	0.181001	0.041001	- 0.001001
0500	0.180947	0.041346	- 0.001537
1000	0.181024	0.041320	- 0.001240
1500	0.181096	0.041258	- 0.001365
2000	0.181101	0.041308	- 0.001326
2500	0.181134	0.041277	- 0.001331
3000	0.181141	0.041289	- 0.001335
3500	0.181151	0.041284	- 0.001330
4000	0.181156	0.041284	- 0.001333
4500	0.181159	0.041284	- 0.001332
5000	0.181160	0.041284	- 0.001332